CHEMISTRY
A EUROPEAN JOURNAL

DOI: 10.1002/chem.200903310

Chemoselectivity as a Delineator of Cuprate Structure in Catalytic 1,4-Addition of Diorganozinc Reagents to Michael Acceptors

Matthias Welker,[a] Simon Woodward,*[a] Luis F. Veiros,*[b] and Maria José Calhorda[c]

Abstract: Reaction of the cyclic thioacetal $(RS)_2CHCHO$ [$R = {}^1/_2 \times -(CH_2)_3-$] with HCCCOMe, followed by treatment with TsCl/DABCO (Ts = tosyl, DABCO = 1,4-diazabicyclo-[2.2.2]octane) affords the mono-protected 1,4-benzoquinone dithioacetal. The reactivity of this SR-protected 1,4-benzoquinone has been compared with the behavior of the analogous OR-protected acetal in copper-catalyzed additions of $ZnMe_2$ by using chiral phosphoramidite ligands. The activation energy for 1,4-methylation of the latter OR-acetals with $ZnMe_2$ (>95% *ee*) has been determined for two CuX_2 precatalysts (X = OAc, 12.2 kcal mol^{-1}; X = OTf, 6.7 kcal mol^{-1}; Tf = triflate). The dithioacetal SR aromatizes in the presence of $Cu^I/ZnMe_2$ giving 1,4-$HOC_6H_4S(CH_2)_3SMe$ through C–S bond formation. The disparate behavior of these two very closely related substrates is in accordance with the formation of closely related cuprate intermediates that were optimized by DFT calculations, supporting the synthetic and kinetic studies and thus defining the mechanisms of both pathways.

Keywords: copper · density functional calculations · P ligands · reaction mechanisms · zinc

Introduction

In 2000 Woodward briefly summarized what was then known about the structures of lithium organocuprates and the mechanisms by which they attack 1,4-Michael acceptors.[1] Through the work of Bertz et al.,[2] Nakamura et al.[3] and others[4] the intimate behavior of lithium homocuprates (e.g., structure **A** in Scheme 1 with X = Me, M = Li, **L*** = no ligand) has indeed emerged from this "black box" towards the rigorously defined picture of Scheme 1. Significant numbers of examples of unligated lithiocuprates that are either characterized by X-ray crystallography (**B**) or by solution NMR spectroscopy (**C**) are now known. Recently, the first Cu^{III} intermediates (**D**) have been characterized by low-temperature "rapid injection NMR" techniques.[2] There remains a dichotomy between experiment and theory: theoret-

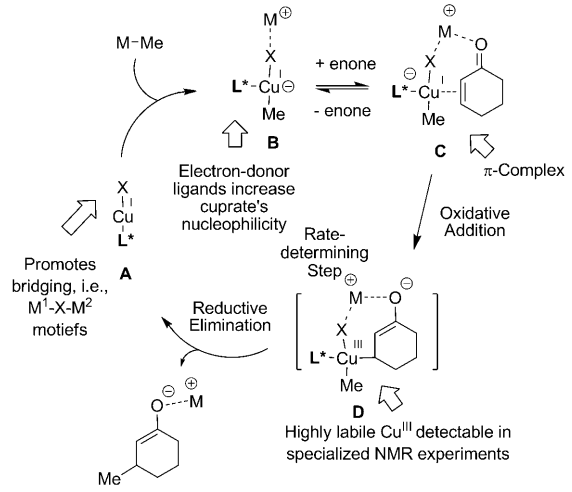

Scheme 1. Simplified mechanism of generalized copper-promoted 1,4-addition of M–Me (M = any suitable counterion) to a representative Michael acceptor (cyclohexenone).

[a] M. Welker, Prof. S. Woodward
School of Chemistry, The University of Nottingham
University Park, Nottingham, NG7 2RD (UK)
Fax: (+44) 115-951-3564
E-mail: simon.woodward@nottingham.ac.uk

[b] Prof. L. F. Veiros
Centro de Química Estrutural, Instituto Superior Técnico
1049-001 Lisboa (Portugal)
Fax: (+351) 21-846-4455
E-mail: veiros@ist.utl.pt

[c] Prof. M. J. Calhorda
Departamento de Química e Bioquímica, CQB
Faculdade de Ciências
Universidade de Lisboa, 1749-016 Lisboa (Portugal)

Supporting information for this article (tables with atomic coordinates for all optimized calculated species, X-ray structural data for compounds: **1a**, **1b**, **3**, and primary kinetic data) is available on the WWW under http://dx.doi.org/10.1002/chem.200903310.

ical approaches suggest that reductive elimination of **D** should be the rate-limiting step of the reaction,[3] yet appreciable concentrations of these species were not found in the reaction mixture.

In a parallel to the investigations for lithiocuprates that are described above, ligand-accelerated[5] copper-catalyzed 1,4-addition of diorganozinc species ZnR_2 (especially R = Me, Et) to cyclohexenone, and related acceptors, has become recognized as the premier method to attain high enantioselectivities.[6] However, the relationship of the stoichiometric lithium cuprate chemistry presented in Scheme 1 to that of the catalytic $Cu^I/ZnMe_2$/**L*** systems (M = ZnMe, **L*** = a phosphoramidite ligand) has remained somewhat obscure. Kinetic studies of chiral copper(I)–phosphoramidite-catalyzed additions of ZnR_2 to enones are limited to early observation of a negative non-linear effect[7] and a recent study of the effect of the ligand structure on the rate by Schrader et al.[8] Additional information on potential interaction modes between the CuX precatalyst and the chiral ligand were gained from comprehensive NMR studies of Gschwind et al.[9]

As the cuprate intermediates in $Cu^I/ZnMe_2$/**L***-promoted reactions are very labile, we sought to harness the power of DFT-based calculations[10] to gain insight into the potential structures of π-complex **C** (M = MeZn, **L*** = phosphoramidite) in this zinc chemistry and their subsequent redox behavior. To maximize the computational robustness of our regime we wished to directly relate our calculations to a predictable "real world" chemistry and were thus attracted to propose differential reactivity of the closely related dienones **1a** and **1b** (Scheme 2).

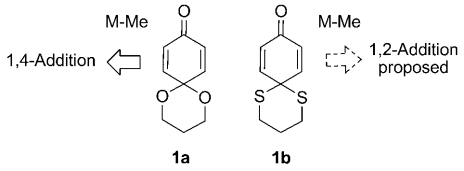

Scheme 2. Literature[11,12] proposed reactivity for dienones **1a** and **b**.

Feringa et al. have demonstrated that **1a** undergoes highly selective *enantiopos* addition of $ZnEt_2$ in the presence of their phosphoramidite.[11] In earlier work Page and coworkers suggested that **1b** reacts with $LiCuMe_2$ by giving an unexpected 1,2-addition product with stoichiometric cuprates.[12] We speculated that the π-complexes formed from **1a** and **1b** that deliver these two disparate products would be highly similar. Further, this common cuprate structure, related to **C**, must be able to accommodate the observed experimental behavior of both, **1a** and **1b**, providing a good test for the validity of any computationally-derived intermediates on the conjugate addition pathway.

Results and Discussion

Synthesis and properties of dienones 1a and 1b: Compound **1a** is available in good yield by a published short synthesis.[11] In our hands, following the six-step procedure by Page et al.[12] for **1b** gave the product, although one $ZnCl_2$-promoted step was capricious (as Page had noted), which limited our overall yields to <10%. Unfortunately, **1b** was not available from reaction of **1a** with 1,3-propane dithiol under all conditions attempted. Alternative products in thiol reactions of benzoquinone acetals have been noted before.[13] As we wished to access significant quantities of **1b** for reactivity studies we designed an alternative route (Scheme 3).

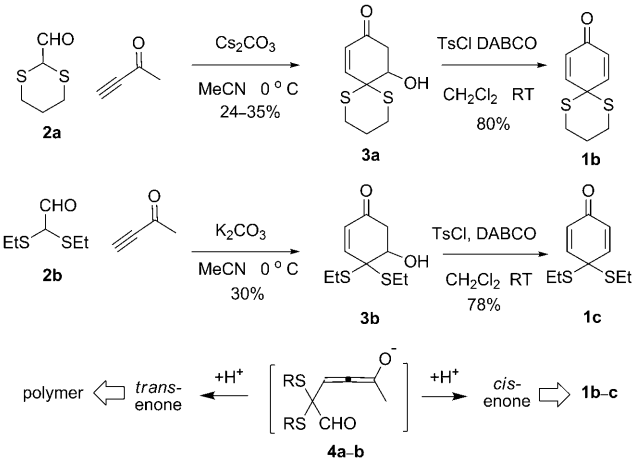

Scheme 3. Alternative route to dieneones **1b** and **c** (Ts = 4-tolylsulfonyl; DABCO = 1,4-diazabicyclo[2.2.2]octane).

Formylation of 1,3-dithiane by using BuLi followed by DMF and aqueous workup provided **2a** in good isolated yield (79%). Direct reaction of crude or distilled **2a** with butyn-2-one led to low yields of **3a** (24–35%). Use of the known[14a] self-dimerization product of **2a** led to similar yields. The poor performance of the reaction is probably a consequence of the initially formed allenoate **4a** that is more successfully protonated to give an undesired *trans*-enone that cannot subsequently cyclize. The formation of **3a** was confirmed by X-ray crystallography as it shows an unexpectedly weak ν(O–H) stretch vibration in its IR spectrum.[14b] Under E_{1cb} elimination conditions **1b** was formed smoothly. The overall three-step process for **1b** is convenient if not high yielding (15–22%). The related monocyclic dienone **1c** was also prepared by an equivalent route for reaction comparison studies (see later). Key ^{13}C NMR spectroscopic, X-ray structural and computational data for the Michael acceptors **1a** and **1b** are compared in Table 1. Electronically and structurally the substrates **1a** and **1b** are closely related; the most significant differences are found in the C–S bond length in **1b** (≈1/3 longer than its *O*-acetal analogue) and the higher chemical shift of the acetal carbon in **1a**.

Table 1. Properties of substrates **1a** and **b** relevant for addition chemistry.

Property	**1a**	**1b**
^{13}C NMR shifts [ppm][a]		
C(1)	185.2	183.8
C(2)	128.5	127.0
C(3)	141.9	146.0
C(4)	89.0	45.3
atomic charge (NPA)[b]		
C(1)	+0.500	+0.490
C(3)	−0.173, −0.222	−0.197, −0.210
structural data [Å][c]		
O−C(1)	1.224	1.230
C(1)−C(2)	1.474	1.464
C(2)−C(3)	1.322	1.328
C(3)−C(4)	1.509	1.497
C(4)−Y (Y = O,S)	1.422	1.831

[a] Determined at 100 MHz in $CDCl_3$ at ambient temperature. [b] Determined by DFT calculations at the PBE1PBE/6-31G** level; the two values at C(3) indicate the two β-carbon atoms. [c] Determined from X-ray crystallographic studies of **1a** and **b**; where two identical bonds were present, an average value is given.

Reactions of dienones 1a and 1b with carbon nucleophiles: In order to attain a direct comparison of the reactivity of **1a** and **1b** both compounds were treated with $ZnMe_2$ under identical catalytic conditions ($Cu(OTf)_2$ (2 mol%, Tf = triflate), CH_2Cl_2, −20 °C for 4 h followed by 0 °C for 1 h) by using the same phosphoramidite $\mathbf{L_A}$ (4 mol%) (Scheme 4).

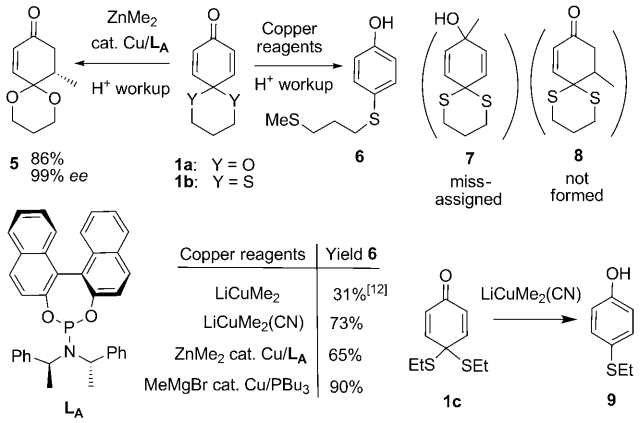

Scheme 4. Real and fictional products that result from organomethyl additions to dienones **1a–c**.

The two-stage temperature profile was needed to attain complete conversion of both compounds. Dienone **1a** gave the expected[11] 1,4-addition product **5** with high enantioselectivity. This behavior was identical when copper(I)thiothene carboxylate (TC) [Cu(TC)][15] or $Cu(OAc)_2$ were used as precatalysts. Equivalent $ZnMe_2/Cu^I/\mathbf{L_A}$-mediated reaction of **1b** gave a product that was identical in every way to the product that results from the reaction of **1b** and $LiCuMe_2$ as described by Page et al.[12] Based on ^{1}H NMR and IR spectroscopic data alone these authors had assigned the 1,2-addition structure **7** to this product. We believe this is a structural misassignment of compound **6** for the following reasons:

1) The ^{13}C NMR data of the product from the reaction of **1b** and $LiCuMe_2$ shows two clear *ipso* aromatic environments but no quaternary signal in the region expected for an sp^3 *C*−O carbon.
2) The methyl signal of the product shows no long-range cross peak to any potential quaternary *C*−O signal in the HMQC spectrum but instead shows a valid cross peak to one of the CH_2−S signals.

Our proposal is confirmed by the reaction of related **1c** with $LiCuMe_2(CN)$ that leads to known **9**.[16] Optimal yields of **6** were attained with MeMgBr addition to **1b** under $CuBr{\cdot}SMe_2/PBu_3$ catalysis (5 mol% each). For rapid formation of **5** the presence of cuprate reagents or copper catalysts was mandatory in all reactions. In no case was any **8** formed within the limits of NMR detection in the crude mixture. Control reactions revealed that the presence of $Cu^I/\mathbf{L_A}$ is required for $ZnMe_2$-induced transformations of **1a** and **1b** to **5** and **6**.

Computational screening for a $ZnMe_2$-derived π-complex ground state: We have used lower levels of computational theory to provide insights into the speciation of labile copper(I) species in Cu-catalyzed reactions of organoaluminiums by simple metal–ligand combination trials.[17] As this approach had been quite successful for aluminium cuprates, a similar method was applied to the problem of assessing the viability of potential zinc cuprates and their π-complexes related to **B** and **C**, respectively (Scheme 1). Acetate was selected as a suitable "computationally small" bridging ligand as triflate was considered to have a too great potential to introduce computational (S) or coordination (O,F) complexities. Studies were carried out by using the PBE1PBE hybrid functional and a VDZP basis set with the core electrons of the metal atoms Cu and Zn described by pseudo-potential functions (see Computational Details). Computational combination of Cu(OAc), $ZnMe_2$ and ligand $\mathbf{L_B}$ (used as a simplified form of phosphoramidite $\mathbf{L_A}$) led to exothermic formation of zinc cuprate $\mathbf{B_1}$ for which dimerization to cuprate $\mathbf{B_2}$ was energetically viable with an energy balance of $\Delta G = 2.3$ kcal mol^{-1} (Scheme 5).

The validity of suitable ground-state π-complexes of zinc cuprates $\mathbf{B_1}$ and $\mathbf{B_2}$ was tested in a wide range of docking experiments with dienone **1a** that lead to the mono- or dicopper π-complexes $\mathbf{C_1}$–$\mathbf{C_6}$ (Scheme 6) by using the same PBE1PBE hybrid functional approach. In one case ($\mathbf{C_1}$) an additional equivalent of $[Cu(OAc)(\mathbf{L_B})_2]$ was included to test a recent mechanistic proposal by Gschwind.[9] In two other cases ($\mathbf{C_2}$ and $\mathbf{C_3}$) an additional equivalent of $\mathbf{L_B}$ or $ZnMe_2$ was included to test recent mechanistic suggestions by Schrader.[8] In all but one case ($\mathbf{C_1}$), very significant increases of the ground-state energy are encountered—these are highly unlikely compatible with the observed efficient catalysis at low temperatures. The closest energetic species

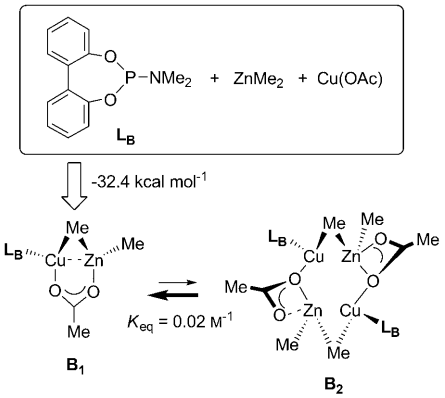

Scheme 5. Lowest energy zinc cuprates accessible from phosphoramidite ligated $\mathbf{L_B}$ and Cu(OAc) in the presence of $ZnMe_2$.

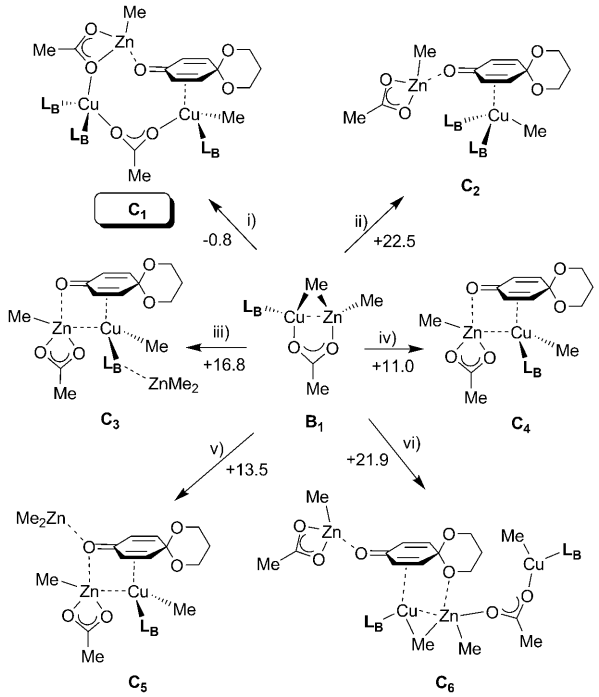

Scheme 6. Dienone (**1a**) docking experiments with zinc cuprate $\mathbf{B_1}$. The numbers (−0.8 to +22.5) indicate the free-energy costs, in kcal mol^{-1}, associated with the transformations: i) $\mathbf{B_1}+\mathbf{1a}+[Cu(OAc)(\mathbf{L_B})_2]$, ii) $\mathbf{B_1}+\mathbf{1a}+\mathbf{L_B}$, iii) $\mathbf{B_1}+\mathbf{1a}+ZnMe_2$, iv) $\mathbf{B_1}+\mathbf{1a}$, v) $\mathbf{B_1}+\mathbf{1a}+ZnMe_2$ (carbonyl bound), and vi) dimerization of $\mathbf{B_1}$, followed by addition of **1a** ($\mathbf{B_2}+\mathbf{1a}$).

to $\mathbf{B_1}$ is π-complex $\mathbf{C_1}$, which is essentially identical to the proposal of Gschwind for the catalyst rest state in 1,4-additions to cyclohexenone.[9]

On the basis of kinetic experiments on $ZnEt_2$ additions to cyclohexenone performed in 2004,[8] Schrader et al. had suggested a structure equivalent to $\mathbf{C_2}$. However, this looks unlikely to be attained in our case due to its relative instability compared to the enone and/or ligand dissociation. Schrader and co-workers also proposed a species closely related to $\mathbf{C_3}$ but with a 5-coordinate copper center that bridges in an $[L_nCu(\mu\text{-}Me)_2ZnMe]$ motif. We could not attain this species. When thus placed, the $ZnMe_2$ unit "slipped", becoming weakly associated with the phosphoramidite ligand ($\mathbf{C_3}$), dissociated completely ($\mathbf{C_4}$), or migrated to the carbonyl oxygen ($\mathbf{C_5}$). No easily energetically accessed π-complex could be attained from interaction of the dimer $\mathbf{B_2}$ with dienone **1a**. Only the high-energy complex $\mathbf{C_6}$ was calculated despite attempts to constrain the π bonds in **1a** to bind both copper centers. The presence of additional $ZnMe_2$ did not improve stability of $\mathbf{B_2}+\mathbf{1a}$, only a weak Lewis acid interaction in the region of the carbonyl group was calculated (structure $\mathbf{C_7}$, 28.6 kcal mol^{-1} above $\mathbf{B_1}$, not shown).

By using the energetically most accessible $\mathbf{C_1}$ as a starting point, attempts were made to profile the putative rate-determining oxidative addition/reductive elimination steps equivalent to "**D** transition states" (Scheme 1) and to rationalize the different chemoselectivity between **1a** and **1b**. Preliminary calculations revealed that the B3LYP functional provides a better description of the energy barrier associated with the formation of **5**, than the one obtained with the PBE1PBE functional (see Computational Details). Thus, all mechanistic studies reported below were obtained with the B3LYP functional. Because of the large "computational size" of these multi-metal species and the demands of transition-state calculations, the structure of the phosphoramidite ligand was further simplified to $(MeO)_2PNMe_2$ ($\mathbf{L_C}$) in the mechanistic calculations. Two isomers of the π-complex with substrate **1a** were optimized, differing on the spacial arrangement around the Cu center. In one isomer the methyl group is close to the six-membered acetal ring ($\mathbf{C_1}'$); this was arbitrarily set as the energy reference compound ($E_{\mathbf{C_1}'}=0.00$ kcal mol^{-1}, see Scheme 7). In the other isomer, $\mathbf{C_1}$, the methyl and phosphoramidite ligand have exchanged positions and, thus, the methyl ligand is on the same side of the carbonyl group. $\mathbf{C_1}$ is 2.2 kcal mol^{-1} less stable than $\mathbf{C_1}'$. The geometry around the Cu center makes $\mathbf{C_1}'$ the starting point for the 1,4-addition, while $\mathbf{C_1}$ provides the reagent for the 1,2-addition. The energy profiles calculated for both reactions are represented in Scheme 7.

Pleasingly the π-complex $\mathbf{C_1}'$ evolves smoothly to the expected enolate product $\mathbf{E_1}$ in a highly exothermic reaction. A clear transition state $\mathbf{D_1}$ could be identified. In the transition state, $\mathbf{D_1}$, methyl migration from the Cu atom to the C_6 ring is under way. The Cu–C(Me) distance (2.136 Å) is already 0.14 Å longer than the corresponding one in $\mathbf{C_1}'$, but the formation of the new C–C bond is only beginning with a separation of 2.211 Å, still far from the value observed in the product, $\mathbf{E_1}$ (1.540 Å). These results are fully corroborated by the corresponding Wiberg indices (WI).[18] The Wiberg index associated with the Cu–C(Me) bond drops from 0.33 in $\mathbf{C_1}'$, to 0.13 in $\mathbf{D_1}$, while for the new C–C bond the corresponding Wiberg index rises from 0.60 in the transition state $\mathbf{D_1}$, to 1.00 in the product $\mathbf{E_1}$, demonstrating that the processes of bond forming and of bond breaking are well advanced when the transition state is reached. Enolate formation is also evident in $\mathbf{E_1}$, with a C–O bond ($d=1.286$ Å, WI = 1.32) that is longer and weaker than the C=O

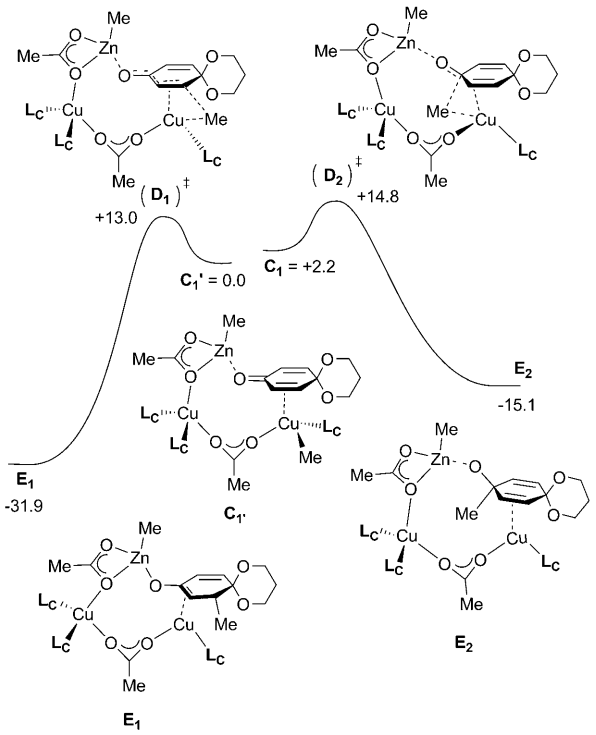

Scheme 7. Calculated free energy profiles of 1,4- and 1,2-additions with substrate **1a**.

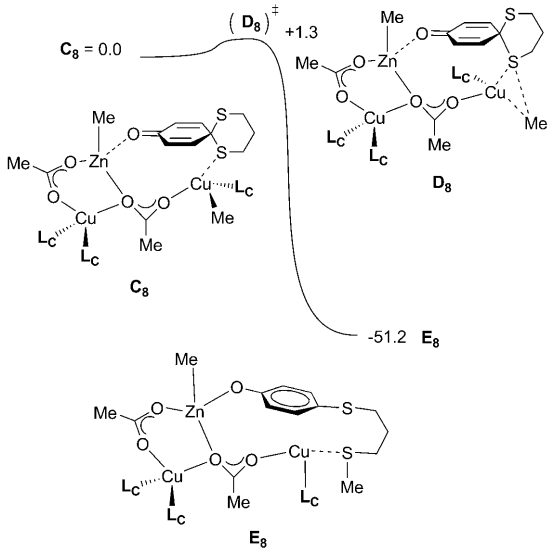

Scheme 8. Calculated free energy profile for the aromatization of **1b** through S–Me bond formation from $\mathbf{C_8}$.

bond present in the $\mathbf{C_1'}$ ($d=1.274$ Å, WI = 1.38). Naturally, the adjacent C–C bond shows the reverse evolution shortening from 1.426 Å (WI = 1.25) in $\mathbf{C_1'}$ to 1.408 Å (WI = 1.44) in $\mathbf{E_1}$.

Alternative reaction pathways to the 1,4-addition were investigated. The energetically most accessible was the 1,2-addition via transition state $\mathbf{D_2}$. This is 14.8 kcal mol^{-1} above the starting point for the 1,4-addition ($\mathbf{C_1'}$), thus, corresponding to a less favorable path when compared with the one previously discussed, which is in line with the experimentally observed chemoselectivity. Despite extensive attempts, no viable reaction vector leading to opening of the acetal **1a** by Cu–Me (equivalent to the reactivity of **1b**) could be detected. This is in line with the experimental observations, as no **10** could be identified within NMR detection limits in spectra of the crude reaction mixture.

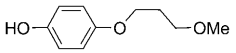

10

Related, but not observed, 1,4- and 1,2-addition reactivity of sulfur dienone **1b** with $ZnMe_2$ was also studied from the sulfur analogues of $\mathbf{C_1'}$ and $\mathbf{C_1}$ ($\mathbf{C_9'}$ and $\mathbf{C_9}$, respectively; see later). However, in accordance with the experimental, a much more favorable reaction pathway to the aromatization product **6** could be calculated, starting from a closely related intermediate $\mathbf{C_8}$. This species is more stable than $\mathbf{C_9'}$ (by 10.9 kcal mol^{-1}) and generated by Cu^{I} coordination to one sulfur atom of the substrate, rather than to the double bond, which leads to a "slipped" thioether ligand in a slightly different overall spacial arrangement (Scheme 8).

Species $\mathbf{C_8}$ shows a very facile rearrangement to the kinetic aromatization product $\mathbf{E_8}$ via an identified transition state $\mathbf{D_8}$. In $\mathbf{D_8}$, formation of the new S–C(Me) bond is only incipient ($d=3.215$ Å, WI = 0.15). In fact, these values indicate that in $\mathbf{D_8}$, the S–C(Me) interaction is only slightly stronger than in $\mathbf{C_8}$ ($d=3.282$ Å, WI = 0.11). Correspondingly, the process of C–S and Cu–C(Me) bond breaking is only starting, once $\mathbf{D_8}$ is reached. The S–C bond becomes only a little longer and weaker, going from $\mathbf{C_8}$ ($d=2.010$ Å, WI = 0.73) to $\mathbf{D_8}$ ($d=2.076$ Å, WI = 0.65), the same happens with the Cu–C(Me) bond ($\mathbf{C_8}$: $d=2.008$ Å, WI = 0.35; $\mathbf{D_8}$: $d=2.012$ Å, WI = 0.33). These results indicate that $\mathbf{D_8}$ is a rather early transition state.

To allow direct comparison with the behavior of dienone **1a** and the erroneous 1,2-reactivity of **1b** proposed by Page, the barriers associated with potential 1,2- and 1,4-addition of $ZnMe_2$ to the sulfur analogues $\mathbf{C_9'}$ and $\mathbf{C_9}$ were calculated. In both cases viable transition states ($\mathbf{D_9}$ and $\mathbf{D_{10}}$) and products ($\mathbf{E_9}$ and $\mathbf{E_{10}}$) could be identified (Scheme 9). The pathways leading to the kinetic 1,4- ($\mathbf{E_9}$) and 1,2-products ($\mathbf{E_{10}}$) were found to be significantly higher in energy than that for the aromatization ($\mathbf{E_8}$) (Scheme 8).

Kinetic and mechanistic investigation of the reactivity of dienones 1a and 1b: Although the computational models proposed fit exactly to the observed experimental features of the reactivity of substrates **1a** and **1b** we sought to further correlate the calculated energy barriers to real kinetic data. The experiments of Schrader et al. demonstrate, that obtaining full low error bar kinetic analyses/rate laws of these air sensitive systems is demanding.[8] Additionally, although it is

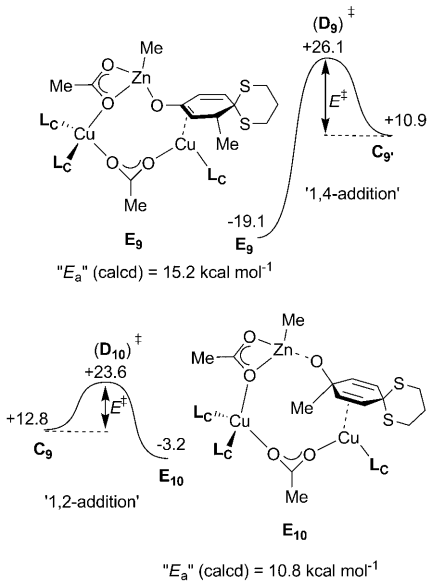

Scheme 9. Calculated free energy profiles for the hypothetical 1,4- and 1,2-additions to **1b**. Structures $\mathbf{C_9}$ and $\mathbf{C_9}'$ are analogous to $\mathbf{C_1}$ and $\mathbf{C_1}'$, respectively, but with bounded **1b** instead of **1a**.

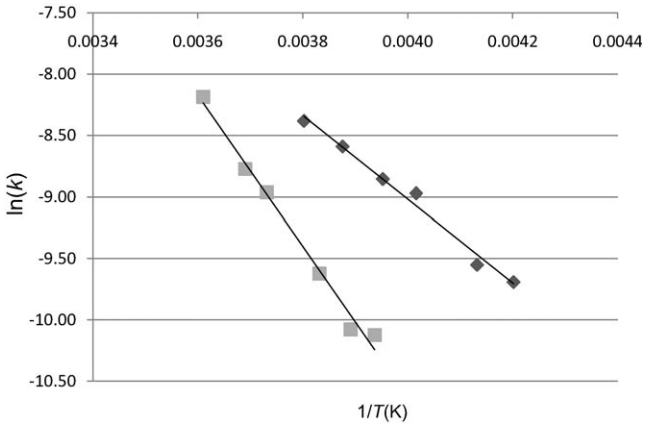

Figure 1. Arrhenius plot of the reaction of **1a** (2.41 mM) with $ZnMe_2$ (2.89 mM) in toluene (18.4 mL), catalyzed by $Cu(OTf)_2$ (grey squares; Tf = triflate) or $Cu(OAc)_2$ (black diamonds) (both at 0.048 mM) and $\mathbf{L_A}$ (0.096 mM). The correlation coefficients for the two data sets are: $R^2(Cu(OAc)_2) = 0.989$ and $R^2(Cu(OTf)_2) = 0.988$.

generally accepted that the transformation of π-complex **C** through intermediate **D** to the product enolate **E** is rate-limiting, it is not known what kinetic advantage this has over other elements of the process. The complex nature of these reaction pathways and the possibilities of mixed copper speciation or even radical reaction pathways[19] means that deceptively simple kinetic results may hide a mélange of effects in this area. Thus, we were attracted to the approach of Krause et al. in measuring a simple Arrhenius "activation energy" for the whole of a cuprate-induced process.[20] Preliminary studies indicated that suitable kinetic data could be attained for the first 2 h of the transformation of **1a** to **5**, catalyzed by $Cu(OAc)_2$ (2 mol %) and $\mathbf{L_A}$ (4 mol %) under the reaction conditions related to those used in the synthetic studies (0.129 M **1a** in toluene, −10 °C, 1.2 equiv $ZnMe_2$). Beyond 2 h (ca. 25 turnovers) the kinetic analyses were invalidated by the generation of minor secondary by-products. Although these did not seem to greatly affect the rate of catalysis, extraction of the concentrations of **1a** and **5** was complicated by GC co-elution and the data were not used. A similar procedure was applied by using $Cu(OTf)_2$ as a copper source, which provided a quicker reaction but lead to similar minor by-products after 2 h. From $Cu(OAc)_2$-catalyzed reactions, conducted at −20 to +5 °C, and $Cu(OTf)_2$-catalyzed reactions, conducted between −35 and −10 °C, two Arrhenius plots could be constructed (Figure 1). In every kinetic run that was investigated the enantioselectivity remained invariant and very high (>95 % *ee*) throughout.

The slope of Figure 1 gives an activation energy (E_a) of 12.2 ± 1.2 kcal mol^{-1} for the $Cu(OAc)_2/\mathbf{L_A}$-catalyzed addition of $ZnMe_2$ to **1a**. Comparison with the calculation presented in Scheme 7 should be made with a degree of caution: a calculated energy barrier for a single step ($\mathbf{C_1}' \rightarrow (\mathbf{D_1})^{\ddagger} \rightarrow \mathbf{E_1}$) suggested to be the rate-determining step, is being compared with E_a for a whole process. Nevertheless, the calculated and experimental results are in good agreement. The fact that a $Cu(OAc)_2$ pre-catalyst is used in the kinetics whereas calculations are performed with Cu(OAc) is irrelevant—it is known that such copper(II) precursors are reduced rapidly under the reaction conditions.[9] It might be expected that increasing the Lewis acidity of the copper complex should engender a faster reaction. This is proven by the fact that the $Cu(OTf)_2/\mathbf{L_A}$-catalyzed reaction shows a reduced activation energy of 6.7 ± 0.7 kcal mol^{-1}. By assuming that Arrhenius plots of the 1,4-addition processes can be equated to the Eyring–Polanyi equation[21] [Eq. (1)], estimates of the activation enthalpies and entropies can be attained.

$$\ln\frac{k}{T} = \frac{-\Delta H^{\ddagger}}{R}\frac{1}{T} + \ln\frac{k_B}{h} + \frac{\Delta S^{\ddagger}}{R} \qquad (1)$$

Values of $\Delta H^{\ddagger} = +11.7$ and $+6.3$ kcal mol^{-1} were determined for the $Cu(OAc)_2$- and $Cu(OTf)_2$-catalyzed processes, respectively. For the activation entropies the determined values of $\Delta S^{\ddagger}$ for the acetate and triflate were −32.5 e.u.[22] and −43.3 e.u., respectively. The observation of significant negative values of $\Delta S^{\ddagger}$ is normally associated with the presence of significant ordering in a transition state. This is also in line with the presumption two coppers, three chiral ligands, one zinc, and the Michael acceptor must all be assembled in the transition state presented here.

It was not possible to compare the kinetic behavior of **1a** with the related dithioacetal **1b**. Despite many attempts we could not attain kinetic data of sufficient quality. The major problem is the lower solubility of the kinetic product **6** of the reaction, which quickly leads to coprecipitation of **6** and **1b**, which is itself highly crystalline. In view of these problems and the predicted, very low, activation energy (1.3 kcal mol^{-1}, see Scheme 8) associated with this transformation an alternative approach was sought. Cleavage of the C–S acetal

bond in **1b** could in principle be driven by two factors: 1) the additional energy generated through aromatization on route to product **6**; or 2) the intrinsically weaker nature of the C–S bond. We conceived that reaction of the monoenone dithioacetal **11** with $ZnMe_2$ might resolve this issue (Scheme 10). However, in practice **11** (also available through literature procedures[12]) showed insufficient reactivity in copper(I)/$\mathbf{L_A}$- or copper(I)/$\mathbf{L_D}$-catalyzed addition of

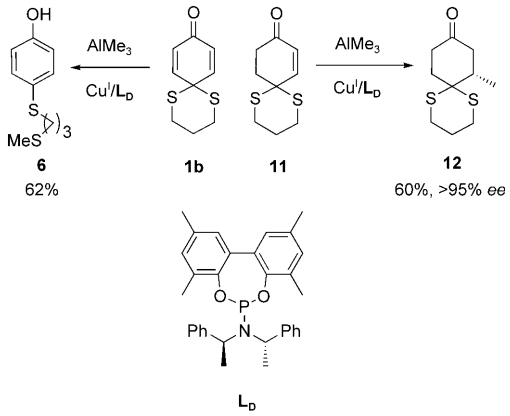

Scheme 10. Copper thiophenecarboxylate/$\mathbf{L_D}$-catalyzed additions to **1a** and **11**. Conditions: $AlMe_3$ (1.5 equiv), [Cu(TC)] (2 mol%; TC = thiothene carboxylate), $\mathbf{L_D}$ (4 mol%), CH_2Cl_2, −78 to −50 °C over 4 h.

$ZnMe_2$ under all conditions tried. However, use of the more Lewis acidic $AlMe_3$ led to sole formation of **12** in >95% *ee* (optimal 60% isolated yield by using $\mathbf{L_D}$), whereas under identical conditions **1b** still afforded **6** as the sole product in 62% isolated yield. The viability of 1,4-addition to **11** indicates that aromatization is the most likely driving force for the formation of **6**. For now we reserve comment on the structure of the π-complexes and transition states involved in the formation of **12**. It is likely that their structures are closely related to the zinc species presented here and this is under current investigation in our laboratories.

Conclusion

The divergent reactivity of the *O*,*O*-acetaldienone **1a** and its dithio analogue **1b** has been resolved by a combination of experimental and DFT procedures. Whereas the former results in highly enantioselective 1,4-addition with Cu^I–phosphoramidite catalysis, the latter leads to S–Me bond formation and aromatization to **6** with exactly the same catalyst system. A confusion in the literature where **6** had been misassigned as the 1,2-addition product **7** has been corrected. Theoretical simulation has shown that very closely related zinc cuprates can account for the reactivity change. This strongly supports the involvement of a common [Zn(μ-X)Cu(μ-X)CuR] motif in all these catalytic reactions (X = a suitable bridging ligand, e.g., OAc, OTf, thiophene carboxylate; Tf = triflate). In the present case, whereas the acetal-substituted Michael acceptor binds through a π-contact to the cooper, the dithioacetal binds through a Cu^I···thioether contact. The origin of the switch in chemoselectivity between **1a** and **1b** can probably be best ascribed to a stronger Cu···Y interaction in the π-complex of the thioacetal (**1b**, Y = S), when compared to the equivalent species for the acetal (**1a**, Y = O). The enhanced donor capability of the S atom, when compared to its O counterpart, is illustrated by the larger coefficients on the sulfur atoms in comparison to the oxygen atoms on the relevant orbitals of substrates **1b** and **1a**, respectively (Figure 2).

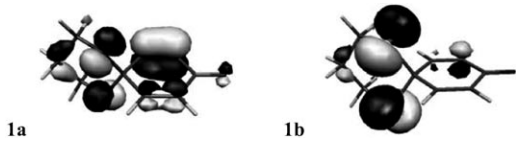

Figure 2. Calculated HOMO−1 orbital for substrate **1a** (*O*,*O*-acetal, left) and HOMO orbital for substrate **1b** (*S*,*S*-dithioacetal, right).

Experimental Section

General: Infrared spectra were recorded by using Perkin–Elmer 983 G infrared and Perkin–Elmer 882 infrared spectrophotometers, or a Bruker IFS 66 spectrometer. ^1H and ^{13}C NMR spectra were recorded on Bruker (AM400, AV400, or DRX 400) or JEOL (JNM-GX270) spectrometers by using $CHCl_3$ ($\delta = 7.27$ ppm) and tetramethylsilane ($\delta = 0.00$ ppm) as standard; *J* values are given in Hz. All spectra were recorded at ambient temperature unless otherwise noted. Mass spectra were obtained on Finnigan-MAT 1020 or Autospec VG (electron impact ionization, EI), Finnigan-QMS (electrospray ionization, ESI), VG-ZAB, or Finnigan MAT 8200 insturments (EI, 70 eV). GC analyses were attained by using an autosampler-equipped Varian 430GC (He carried gas, flow rate 1.5 mL min^{-1}) under the conditions and columns described for each compound Optical rotations were measured on Bellingham Stanley ADP 440 in units of 10^{-1} deg cm^2 g^{-1}; concentration (*c*) is given as g 100 cm^{-3}. All reactions involving air sensitive materials were carried out under an argon atmosphere by using standard Schlenk techniques. Reaction solvents were distilled under argon from appropriate agent immediately prior to use. Petroleum ether refers to the fraction with b.p. 40–60 °C. The following compounds were attained by literature procedures: **1a**,[11] **1b**,[12] $\mathbf{L_A}$,[17] **2a**,[14] **11**,[12] and $\mathbf{L_D}$.[23]

Alternative preparation of 1b–c

2-Formyl-1,3-dithiane (2a):[14] To a flame-dried flask containing 1,3-dithiane (2.50 g, 20.8 mmol) in dry THF (50 mL) at −30 °C *n*BuLi (14.0 mL, 1.6 M in hexane, 22.4 mmol) was added and the reaction mixture was stirred at this temperature for 1 h. The mixture was allowed to come to −10 °C and dry *N*,*N*-dimethylformamide (560 μL, 7.21 mmol) was added. The mixture was stirred for 2 h at −10 °C before warming to 0 °C and overnight stirring at room temperature. The resulting suspension was poured into ice water (50 mL) and the mixture was extracted with pentane (20 mL) several times. The aqueous layer was neutralized with hydrochloric acid (1 M) and then extracted several times with diethyl ether (20 mL). The total organic fractions were combined, dried ($MgSO_4$), filtered, and concentrated in vacuo. The crude product was used without further purification or distilled under reduced pressure (80–90 °C at 1 mmHg) to give the desired compound as an unstable colorless oil (1.85 g, 60%) with literature properties.[14] ^1H NMR (270 MHz, $CDCl_3$, 25 °C): $\delta = 9.47$ (s, 1H; C*H*=O), 4.09 (s, 1H; C*H*CH=O), 3.05–2.83 (m, 2H; SCH_2), 2.57–2.46 (m, 2H; SCH_2), 2.09–1.88 ppm (m, 2H;

CH_2); ^{13}C NMR (68 MHz, $CDCl_3$, 25 °C): δ = 188.2, 47.5, 25.3, 24.7 ppm (2C); IR ($CHCl_3$ solution): $\tilde{\nu}$ = 2909, 2821, 1716, 1672, 1386, 1280, 1093, 1001, 907 cm^{-1}; MS (EI+): *m/z* (%): 148.00 (15) $[M]^+$, 119.00 (100), 75.03 (12).

2,2-Bis(ethylthio)acetaldehyde (2b): To a solution of 40% glyoxal in water (387 μL, 33.75 mmol) and ethanethiol (5 mL, 67 mmol; **STENCH!**) a solution of HCl (2 M, 0.4 mL) was added at room temperature. The heterogeneous mixture turned to white after 15 min and was then stirred vigorously overnight. The organic phase was separated and the aqueous phase was extracted with CH_2Cl_2 (2×10 mL) and the combined organic phases were washed once with dilute aqueous solution of Na_2CO_3. The organic layer was filtered through a cotton plug and the bulk of the solvent was removed by distillation at atmospheric pressure (40 °C) Light petrol (b.p. 40–60 °C, 5 mL) was added and distillation was resumed to ensure the residual oil was free from noxious ethanethiol. The residual oil was then distilled under reduced pressure (70–75 °C at 1 mmHg) to afford the desired product as a colorless oil (2.21 g, 40%). ^{1}H NMR (270 MHz, $CDCl_3$, 25 °C): δ = 9.17 (d, *J* = 4.2 Hz, 1H; C*H*=O), 4.23 (d, *J* = 4.2 Hz, 1H; C*H*–S), 2.60 (dq, *J* = 7.4, 3.9 Hz, 4H; CH_2), 1.26 ppm (t, *J* = 7.4 Hz, 6H; CH_3); ^{13}C NMR (75 MHz, $CDCl_3$, 25 °C): δ = 189.3, 55.8, 24.8 (2C), 14.5 ppm (2C); IR ($CHCl_3$ solution): $\tilde{\nu}$ = 2976, 2932, 2875, 2828, 2709, 1712, 1453, 1424, 1379, 1267, 1053, 1020, 978, 827 cm^{-1}; HRMS (EI): *m/z*: calcd for $C_6H_{12}OS_2$: 164.032959 $[M]^+$; found: 164.033660.

11-Hydroxy-1,5-dithiaspiro[5.5]undec-7-en-9-one (3a): Freshly distilled 2-formyl-1,3-dithiane (**2a**) (500 mg, 3.37 mmol) in acetonitrile (6 mL) was added in a flame-dried Schlenk tube under argon. But-3-yn-2-one (275 mg, 4.05 mmol) and K_2CO_3 (1.09 g, 3.37 mmol) were successively added to this solution at room temperature. The resulting yellow solution was cooled to 0 °C, stirred, and allowed to come to room temperature overnight. The mixture turned slowly red–orange in color. The reaction was quenched with saturated aqueous solution of NH_4Cl, extracted with CH_2Cl_2, dried ($MgSO_4$), and concentrated in vacuo. The crude mixture was purified by flash chromatography (petroleum ether/Et_2O 2:1) to give the desired product as an orange solid (0.263 g, 36%). R_f = 0.15 (petroleum ether/Et_2O 1:1); m.p. 97–98 °C; ^{1}H NMR (270 MHz, $CDCl_3$, 25 °C): δ = 6.62 (dd, *J* = 10.8 Hz, 2.0 Hz, 1H; =C*H*CO), 6.00 (d, *J* = 10.8 Hz, 1H; C*H*=CHCO), 4.55 (t, *J* = 2.4 Hz, 1H; C*H*OH), 3.14–2.70 (m, 6H), 2.20–1.80 ppm (m, 2H); ^{13}C NMR (100 MHz, $CDCl_3$, 25 °C): δ = 195.8, 144.7, 129.4, 69.5, 53.4, 41.1, 27.0, 25.1, 23.2 ppm; IR ($CHCl_3$ solution): $\tilde{\nu}$ = 3484, 2913, 1689, 1602, 1383, 1082, 1056, 875 cm^{-1}; MS (EI+):: *m/z* (%): 216.03 (37.1) $[M]^+$, 172.00 (100), 115.97 (22.0), 97.98 (14.9).

4,4-Bis(ethylthio)-5-hydroxycyclohex-2-enone (3b): Preparation of **3b** was performed in an equivalent manner to **3a** from aldehyde **2b** (2.00 g, 12.17 mmol) dissolved in acetonitrile (15 mL) and butyn-2-one (994 mg, 14.60 mmol) followed by addition of a single portion of K_2CO_3 (1.68 g, 12.17 mmol). Crude **3b**, an oil, was purified by column chromatography (petroleum ether/Et_2O 2:1) to afford the desired compound as a yellow liquid (678 mg, 24%). R_f = 0.20 (petroleum ether/Et_2O 1:1); ^{1}H NMR (400 MHz, $CDCl_3$, 25 °C): δ = 6.70 (dd, *J* = 10.1, 0.7 Hz, 1H; C*H*=CHCO), 5.95 (d, *J* = 10.1 Hz, 1H; CH=C*H*-CO), 4.12 (t, *J* = 6.3 Hz, 1H; C*H*-OH), 3.22 (s, 1H; O*H*), 2.84–2.82 (m, 2H; CH_2), 2.78–2.57 (m, 4H; CH_2S), 1.21 ppm (dt, *J* = 7.5, 1.6 Hz, 6H; CH_3); ^{13}C NMR (100 MHz, $CDCl_3$, 25 °C, TMS): δ = 196.4, 148.4, 128.6, 71.1, 62.8, 42.4, 24.1, 23.3, 14.2 (2C) ppm; IR ($CHCl_3$ solution): $\tilde{\nu}$ = 3534, 3009, 2976, 3932, 2874, 1684, 1611, 1449, 1379, 1341, 1300, 1265, 1240, 1163, 1088, 1057, 975, 909, 859, 822 cm^{-1}; MS (ES+): *m/z* (%): 487.11 (10), 419.08 (22), 256.05 (10), 255.05 $[M+Na]^+$ (100), 233.07 $[M+H]^+$ (3), 171.05 (68); HRMS (ES+): *m/z*: calcd for $C_{10}H_{16}O_2S_2$: 255.04839 $[M+Na]^+$; found: 255.0474.

1,5-Dithiaspiro[5.5]undeca-7,10-dien-9-one (1b): A solution of alcohol **3a** (160 mg, 0.74 mmol) and DABCO (166 mg, 1.48 mmol) in CH_2Cl_2 (3 mL) was stirred at room temperature for 5 min. Solid TsCl (212 mg, 1.12 mmol) was added in a single portion. The resulting orange mixture was stirred at room temperature for 4 h. The reaction conversion was monitored by TLC (petroleum ether/Et_2O 2:1). An aqueous solution of $NaHCO_3$ (10 mL) was added and the product was extracted with CH_2Cl_2 (4×10 mL). The combined organic phases were dried ($MgSO_4$) and concentrated in vacuo. The crude oil was purified by column chromatography (petroleum ether/Et_2O 2:1) to afford **1b** as a beige solid (117 mg, 80%), which is stable for weeks when kept under argon in freezer. R_f = 0.30 (petroleum ether/Et_2O 1:1); m.p. 58–60 °C; ^{1}H NMR (400 MHz, $CDCl_3$, 25 °C): δ = 7.19 (d, *J* = 10.0 Hz, 2H; C*H*=CHCO), 6.23 (d, *J* = 10.0 Hz, 2H; CH=C*H*CO), 3.01 (m, 4H; S$CH_2CH_2CH_2$S), 2.09 ppm (m, 2H; SCH_2CH_2 CH_2S); ^{13}C NMR (100 MHz, $CDCl_3$, 25 °C): δ = 183.8, 146.0 (2C), 127.0 (2C), 45.3, 26.2 (2C), 23.2 ppm; IR ($CHCl_3$ solution): $\tilde{\nu}$ = 2912, 2360, 1662, 1620, 871 cm^{-1}; MS (EI): *m/z* (%): 313.91 (47), 198.02 $[M]^+$ (100), 156.96 (30), 124.00 (14), 74.02 (24). This material had identical properties to that prepared by the six-step synthesis described by Page et al.[12]

4,4-Bis(ethylthio)cyclohexa-2,5-dienone (1c): A solution of alcohol **3b** (145 mg, 0.62 mmol) and DABCO (140 mg, 1.25 mmol) in CH_2Cl_2 (1.5 mL) was stirred at room temperature for 5 min. Solid TsCl (179 mg, 0.94 mmol) was added in a single portion. The resulting orange mixture was stirred at room temperature for 4 h. The reaction conversion was monitored by TLC (petroleum ether/Et_2O 2:1). An aqueous solution of $NaHCO_3$ (5 mL) was added and the product was extracted with CH_2Cl_2 (4×10 mL). The combined organic phases were dried ($MgSO_4$) and concentrated in vacuo. The crude oil was purified by column chromatography (petroleum ether/Et_2O 2:1) to afford **1c** as a dark oil (103 mg, 78%). R_f = 0.48 (petroleum ether/Et_2O 2:1); ^{1}H NMR (400 MHz, $CDCl_3$, 25 °C): δ = 6.88 (d, 2H, *J* = 10.0 Hz, C*H*=CHCO), 6.26 (d, 2H, *J* = 10.0 Hz, CH=C*H*O), 2.47 (q, 4H, *J* = 7.6 Hz, CH_2-S), 1.20 ppm (t, 6H, *J* = 7.6 Hz, CH_3); ^{13}C NMR (100 MHz, $CDCl_3$, 25 °C): δ = 184.6, 149.8 (2C), 128.1 (2C), 53.6, 24.6 (2C), 14.2 ppm (2C); IR ($CHCl_3$, solution): $\tilde{\nu}$ = 3018, 2985, 2923, 23180, 1656, 1612, 869 cm^{-1}; MS (EI): *m/z* (%): 91.1 (15), 105.0 (15), 121.1 (100), 154.0 (22), 214.0 (9); HRMS (EI): *m/z*: calcd for $C_{10}H_{14}OS_2$: 214.0481; found: 214.0483.

Generalized additions of $ZnMe_2$ to 1a–c

(*S*)-11-Methyl-1,5-dioxaspiro[5.5]undec-7-en-9-one (5): A flame-dried Schlenk tube was charged with $Cu(OAc)_2$ (2.6 mg, 2 mol%), ligand $\mathbf{L_A}$ (15.6 mg, 4 mol%), and CH_2Cl_2 (1 mL), under argon. The resulting suspension was stirred for 15 min and the mixture was cooled to −20 °C. A solution of dimethylzinc (1.2 M in toluene, 0.90 mL, 1.08 mmol, 1.5 equiv) was added dropwise and the mixture was stirred for 5 min at −20 °C. After this time, benzoquinone monoacetal **1a** (120 mg, 0.72 mmol) dissolved in CH_2Cl_2 (1 mL) was added dropwise. The resulting yellow solution was stirred at −20 °C for 4 h. The reaction was quenched with NH_4Cl, extracted with Et_2O (20 mL), dried ($MgSO_4$), and concentrated in vacuo to afford a dark oil (113 mg, 87%). Analysis by ^{1}H NMR and GC indicated a conversion of 89% to (*S*)-**5** with 99% *ee*. ^{1}H NMR (400 MHz, $CDCl_3$, 25 °C): δ = 7.35 (d, *J* = 10.4 Hz, 1H; C*H*=CHCO), 6.04 (d, *J* = 10.4 Hz, 1H; =C*H*CO), 4.00–3.90 (m, 4H; O$CH_2CH_2CH_2$O), 2.48–2.42 (m, 3H; C*H*-CH_2), 2.09–2.03 (m, 1H; $OCH_2CH_2CH_2O$), 1.59–1.55 (m, 1H; $OCH_2CH_2CH_2O$), 1.08 ppm (d, *J* = 6.0 Hz, 3H; CH_3); ^{13}C NMR (100 MHz, $CDCl_3$, 25 °C): δ = 199.3, 143.8, 129.9, 95.5, 60.7 (2C), 41,9, 38.9, 25.3, 13.9 ppm; IR ($CHCl_3$ solution): $\tilde{\nu}$ = 2934, 2875, 1682, 1388, 1114, 986 cm^{-1}; MS (EI+): *m/z* (%): 182.10 $[M]^+$ (37), 154.10 (34), 140.05 (49), 124.05 (100), 112.05 (54), 82.00 (41); HRMS (ES+): *m/z*: calcd for $C_{10}H_{14}O_3$: 182.0943 $[M]^+$; found: 182.09433; GC (assay on Lipodex A column, 110 °C isothermal): retention time: 15.0 min ((*R*)-**5**) and 15.2 min ((*S*)-**5**).

Methyl-(3-(*p*-tolylthio)propyl)sulfane (6): A procedure as described for compound **5** was followed by using copper(II)triflate (4.8 mg, 0.013 mmol) and benzoquinone dithioacetal **1b** (130 mg, 0.66 mmol). The reaction was performed in CH_2Cl_2 (2 mL). Upon addition of **1b** the reaction mixture became light brown. After 24 h at −20 °C, no starting material could be detected by TLC. The mixture was quenched with NH_4Cl, filtered through celite to remove some insoluble material, extracted with Et_2O, dried ($MgSO_4$), and concentrated in vacuo to afford **6** as a brown oil (90 mg, 65%). Proton NMR indicated total conversion towards the aromatized product. ^{1}H NMR (400 MHz, $CDCl_3$, 25 °C:) δ = 7.30 (d, *J* = 8.4 Hz, 2H; CH_{ar}), 6.77 (d, *J* = 8.4 Hz, 2H; =CH_{ar}), 5.10 (brs, 1H; O*H*), 2.91 (t, *J* = 7.2 Hz, 2H; CH_2), 2.59 (t, *J* = 7.2 Hz, 2H; CH_2), 2.06 (s, 3H; CH_3), 1.85 ppm (quintuplet, *J* = 7.2 Hz, 2H; CH_2); ^{13}C NMR (100 MHz, $CDCl_3$, 25 °C): δ = 154.9, 133.5 (2C), 126.3, 116.0 (2C), 345, 32.7, 28.3, 15.4 ppm; IR ($CHCl_3$ solution): $\tilde{\nu}$ = 3593, 2919, 1599, 1584, 1493, 1320,

1167, 1094, 960 cm^{-1}; HRMS (ES−): *m/z*: calcd for $C_{10}H_{14}OS_2$: 213.0408 $[M-H]^-$; found: 213.0417. These data are not consistent with the structure **7** proposed in the literature,[12] which is a miss assignment.

4-(Ethylthio)phenol (9): A similar procedure as described for compound **4** was followed, starting from benzoquinone dithioacetal **1c** (195 mg, 0.91 mmol). After 3.5 h, no starting material could be detected by TLC. The mixture was quenched with NH_4Cl, extracted with Et_2O, dried ($MgSO_4$), and concentrated in vacuo to afford the product as a yellow solid (99 mg, 59%). m.p. 38–40 °C; ^{1}H NMR (400 MHz, $CDCl_3$, 25 °C): $\delta = 7.29$ (d, $J = 8.4$ Hz, 2H; CH_{ar}), 6.78 (d, $J = 8.4$ Hz, 2H; CH_{ar}), 2.90 (q, $J = 7.2$ Hz, 2H; CH_2), 1.24 ppm (t, $J = 7.2$ Hz, 2H; CH_3); ^{13}C NMR (100 MHz, $CDCl_3$, 25 °C): $\delta = 154.8$, 133.4 (2C), 126.3, 115.9 (2C), 29.8, 14.6 ppm; IR ($CHCl_3$ solution): $\tilde{\nu} = 3595$, 2929, 1600, 1584, 1494, 1257, 1170 cm^{-1}; MS (EI): *m/z* (%): 97.0 (20), 125.0 (23), 126.0 (26), 139.0 (32), 154.0 (100); HRMS (EI): *m/z*: calcd for $C_8H_{10}OS$: 154.0452; found: 154.0443. This material was identical to an example described in the literature.[16]

7-Methyl-1,5-dithiaspiro[5.5]undecan-9-one (12): A flame-dried Schlenk tube was charged with [Cu(TC)][15] (2.3 mg, 2 mol%), ligand $\mathbf{L_D}$[23] (11.9 mg, 4 mol%), and CH_2Cl_2 (1.0 mL) under argon. The suspension was stirred at room temperature for 15 min and then cooled to −78 °C. Trimethylaluminium (2 M in hexane, 0.45 mL, 0.90 mmol, 1.5 equiv) was added dropwise. The mixture was stirred for 2 min at −78 °C after which time enone **11** (120 mg, 0.60 mmol) dissolved in CH_2Cl_2 (2.0 mL) was added dropwise. The solution turned yellow and was stirred while it was allowed to warm slowly from −78 to −10 °C over 5 h. Complete disappearance of the starting material (followed by TLC, petroleum ether/Et_2O 2:1) was observed. The reaction was quenched with aqueous NH_4Cl, extracted with CH_2Cl_2 (20 mL), dried ($MgSO_4$), and concentrated in vacuo. The crude material was purified by flash chromatography (petroleum ether/Et_2O 2:1) to afford the product as a yellow oil (78 mg, 60% yield, >95% *ee*). The enantiomeric excess was measured by NMR after derivatization with (1*R*,2*R*)-(+)-1,2-dipheneylethylene diamine.[24] $[\alpha]_D^{24} = +10.6$ ($c = 1.00$, $CHCl_3$); ^{1}H NMR (400 MHz, $CDCl_3$, 25 °C): $\delta =$ 3.06 (ddd, $J = 14.4$, 11.2, 3.1 Hz, 1H; CH_{2a}CH$_2$S), 2.91 (ddd, $J = 14.4$, 11.2, 3.1 Hz, 1H; CH_{2a}S), 2.83–2.69 (m, 3H; CH_{2b}-CH$_{2a}$S, CH_{2a}), 2.62–2.51 (m, 1H; CH_{2b}), 2.55 (m, 1H; CHCO), 2.49–2.41 (m, 1H; CH_{2a}), 2.38 (m, 1H; CHCO), 2.35 (m, 1H; CHCH$_3$), 2.21–2.15 (m, 1H; CH_{2b}), 2.15–2.05 (m, 1H; CH_{2b}S), 1.97–1.86 (m, 1H; CH_{2b}S), 1.20 ppm (d, $J = 6.6$ Hz, 3H; CH_3); ^{13}C NMR (100 MHz, $CDCl_3$, 25 °C): $\delta = 209.5$, 53.8, 45.0, 41.6, 38.3, 35.2, 26.3, 24.5, 17.0 ppm; IR ($CHCl_3$ solution): $\tilde{\nu} = 2966$, 2912, 1712, 1453, 1417, 1381, 1340, 1278, 1239, 1143, 909 cm^{-1}; MS (ES+): *m/z* (%): 455.12 (21), 271.08 (12), 240.06 (11), 239.05 $[M+Na]^+$ (100), 217.07 $[M+H]^+$ (14); HRMS (ES+): *m/z*: calcd for $C_{10}H_{16}OS_2$: 239.05348 $[M+Na]^+$; found: 239.0538.

Kinetic studies of the addition of $ZnMe_2$ to 1a: The kinetic measurements were performed under an argon atmosphere in a flame-dried round bottom flask. The temperature was controlled by a cold thermometer from Brannan and was maintained constant within ±0.5 K by using a Thermo Haake DC50K75 cryostat. A solution of ligand $\mathbf{L_A}$ (65 mg, 4 mol%) and $Cu(OAc)_2$ (11.7 mg, 2 mol%) in freshly distilled toluene (16.0 mL) was prepared and stirred at room temperature for 30 min. After that time the solution was cooled to the appropriate temperature and diethylzinc (1.2 M in toluene, 3.26 mL, 3.91 mmol) was added to the reaction mixture. At the timepoint $t = 0$, a previously cooled solution of dienone **1a** (500 mg, 3.00 mmol) in toluene (4.0 mL) was added to the reaction mixture (end volume: 23.26 mL, starting concentration of **1a**: 0.129 M). Aliquots were taken under an argon counterflow at regular intervals (by using a Pasteur pipette that had been previously cooled in liquid nitrogen) and immediately hydrolyzed in a pre-cooled mixture of methanol already present in the reaction cooling bath. The organic components were analyzed by gas chromatography (Lipodex A, isothermal 110 °C): retention times: 15.0 min ((*R*)-**5**), 15.2 min ((*S*)-**5**), and 16.0 min (**1a**).

Computational Details

The calculations were performed by using the Gaussian 03 software package.[25] The PBE1PBE functional was used for the screening of π-complexes (Scheme 6) and for preliminary mechanistic studies. That functional uses a hybrid-generalized gradient approximation (GGA), including 25% mixture of Hartree–Fock[26] exchange with DFT[10] exchange-correlation, given by Perdew, Burke, and Ernzerhof functional (PBE).[27] However, we verified that the energy barrier for 1,4-addition to acetal **1a** calculated with the B3LYP functional (13.0 kcal mol^{-1}) was considerably closer to the experimental activation energy ($E_a = 12.2$ kcal mol^{-1}), than the corresponding value obtained with PBE1PBE (7.2 kcal mol^{-1}). Thus, all mechanistic calculations were repeated by using the B3LYP functional. This is also an hybrid functional, including a mixture of Hartree–Fock exchange (20%) with DFT exchange correlation, given by Becke's three-parameter functional with the Lee, Yang, and Parr correlation functional, which includes both local and non-local terms.[28] All calculations were performed without symmetry constraints. The optimized geometries were obtained with the LanL2DZ basis set[29] augmented with an f-polarization function,[30] for Cu and for Zn, and a standard 6-31G(d,p)[31] for the remaining elements. Transition-state optimizations were performed with the synchronous transit-guided quasi-Newton method (STQN) developed by Schlegel et al.[32] Frequency calculations were performed to confirm the nature of the stationary points, yielding one imaginary frequency for the transition states and none for the minima. Each transition state was further confirmed by following its vibrational mode downhill on both sides, and obtaining the minima presented on the energy profiles. The free energy values presented in Schemes 6–9 and discussed along the text were obtained at 298.15 K and 1 atm by conversion of the zero-point-corrected electronic energies with the thermal energy corrections based on the calculated structural and vibrational frequency data. A natural population analysis (NPA)[33] and the resulting Wiberg indices[18] were used for a detailed study of the electronic structure and bonding of the optimized species. The orbital drawings were obtained by using the program MOLEKEL 4.0.[34]

Acknowledgements

M.W. is grateful to the FP6 Programme for providing a Marie Curie Early Stage Fellowship under Contract MEST-CT-2005-019780 (INDACCHEM). Helpful input from the COST D40 Programme on "Innovative Catalysis" and from the UK government (EPSRC grant EP/F033478/1) is acknowledged by S.W. We thank Prof. A. J. Blake and Dr. W. Lewis and Dr. R. Fryatt for their input into the crystallographic and preliminary synthetic studies. M.J.C. thanks FCT and FEDER for financial support (PPCDT/QUI/58925/2004).

[1] S. Woodward, *Chem. Soc. Rev.* **2000**, *29*, 393–401.
[2] a) Detection of copper(III) intermediate "**D**" by NMR: S. H. Bertz, S. Cope, M. Murphy, C. A. Ogle, B. J. Taylor, *J. Am. Chem. Soc.* **2007**, *129*, 7208–7209; b) copper(III) species with coordinated ligands: E. R. Bartholomew, S. H. Bertz, S. Cope, D. C. Dorton, M. Murphy, C. A. Ogle, *Chem. Commun.* **2008**, 1176–1177.
[3] a) Recent key overviews of theoretical approaches: S. Mori, E. Nakamura in *Modern Organocopper Chemistry* (Ed.: N. Krause), Wiley-VCH, Weinheim, **2002**, pp. 315–346. b) Mechanism of $LiCuR_2$ addition to π-extended Michael acceptors: N. Yoshikai, T. Yamashita, E. Nakamura, *Chem. Asian J.* **2006**, *1*, 322–330. c) "Dummy" ligand effects in 1,4-addition: M. Yamanaka, E. Nakamura, *J. Am. Chem. Soc.* **2005**, *127*, 4697–4706.
[4] a) Diastereoselectivity in π-complex formation: W. Henze, T. Gärtner, R. M. Gschwind, *J. Am. Chem. Soc.* **2008**, *130*, 13718–13726. Recent key reviews of cuprate solution structure: b) R. M. Gschwind, *Chem. Rev.* **2008**, *108*, 3029–3053; c) T. Gartner, R. M.

Gschwind in *The Chemistry of Organocopper Compounds* (Eds.: Z. Rappoport, I. Marek), Wiley, New York, **2009**.

[5] D. J. Berrisford, C. Bolm, K. B. Sharpless, *Angew. Chem.* **1995**, *107*, 1159–1170; *Angew. Chem. Int. Ed.* **1995**, *42*, 1059–1070.

[6] Key overviews of development of this area: a) A. Alexakis, J. E. Bäckvall, N. Krause, O. Pàmies, M. Diéguez, *Chem. Rev.* **2008**, *108*, 2796–2823; b) J. Christoffers, G. Koripelly, A. Rosiak, M. Roessle, *Synthesis* **2007**, 1279–1300; c) T. Jerphagnon, M. G. Pizzuti, A. J. Minnaard, B. L. Feringa, *Chem. Soc. Rev.* **2009**, *38*, 1039–1075.

[7] L. A. Arnold, R. Imbos, A. Mandoli, A. H. M. de Vries, R. Naaz, B. L. Feringa, *Tetrahedron* **2000**, *56*, 2865–2878.

[8] T. Pfretzschner, L. Kleenmann, B. Janza, K. Harms, T. Schrader, *Chem. Eur. J.* **2004**, *10*, 6048–6057.

[9] H. Zhang, R. M. Gschwind, *Chem. Eur. J.* **2007**, *13*, 6691–6700.

[10] R. G. Parr, W. Yang, *Density Functional Theory of Atoms and Molecules*, Oxford University Press, New York, **1989**.

[11] a) R. Imbos, M. H. G. Brilman, M. Pineschi, B. L. Feringa, *Org. Lett.* **1999**, *1*, 623–625; b) R. Imbos, M. H. G. Brilman, M. Pineschi, B. L. Feringa, *Org. Lett.* **1999**, *1*, 1873; c) R. Imbos Ph.D. Thesis, University of Groningen (Germany), **2002**.

[12] P. C. Bulman Page, S. A. Harkin, A. P. Marchington, M. B. Van Niel, *Tetrahedron* **1989**, *45*, 3819–3838.

[13] a) P. de March, M. Escoda, M. Figueredo, J. Font, *Tetrahedron Lett.* **1995**, *36*, 8665–8668; b) P. G. Dormer, A. M. Kassim, J. L. Leazer, F. Lang, F. Xu, K. A. Savary, E. G. Corley, L. DiMichele, J. O. DaSilva, A. O. King, D. M. Tschaen, R. D. Larsen, *Tetrahedron Lett.* **2004**, *45*, 5429–5432.

[14] a) A. I. Meyers, R. C. Strickland, *J. Org. Chem.* **1972**, *37*, 2579–2583; b) CCDC-756136 (**1a**), CCDC-756137 (**1b**), and CCDC-756138 (**3**) contain the supplementary crystallographic data for this paper. These data can be obtained free of charge from The Cambridge Crystallographic Data Centre via www.ccdc.cam.ac.uk/data_request/cif.

[15] G. D. Allred, L. S. Liebeskind, *J. Am. Chem. Soc.* **1996**, *118*, 2748–2749.

[16] S. Ghersetti, A. Mangini, F. Taddei, *Annali di Chimica* **1965**, *55*, 358–364.

[17] S. Woodward, *Synlett* **2007**, 1490–1500.

[18] a) K. B. Wiberg, *Tetrahedron* **1968**, *24*, 1083; b) Wiberg indices are electronic parameters related to the electron density between atoms. They can be obtained from a natural population analysis and provide an indication of the bond strength.

[19] For radical effects in 1,4-addition chemistry, see: a) K. Li, A. Alexakis, *Angew. Chem.* **2006**, *118*, 7762–7765; *Angew. Chem. Int. Ed.* **2006**, *45*, 7600–7603; b) S. H. Bertz, *Org. Biomol. Chem.* **2005**, *3*, 392–394.

[20] J. Canisius, A. Gerold, N. Krause, *Angew. Chem.* **1999**, *111*, 1727–1730; *Angew. Chem. Int. Ed.* **1999**, *38*, 1644–1646.

[21] J. C. Polanyi, *Science* **1987**, *236*, 680–690, and references therein.

[22] Non-SI unit of molar entropy used, e.u. = 4.184 $J K^{-1} mol^{-1}$.

[23] M. Vuagnoux-d'Augustin, A. Alexakis, *Chem. Eur. J.* **2007**, *13*, 9647–9662.

[24] A. Alexakis, J. C. Frutos, P. Mangeney, *Tetrahedron: Asymmetry* **1993**, *4*, 2431–2434.

[25] Gaussian 03, Revision C.02, M. J. Frisch, G. W. Trucks, H. B. Schlegel, G. E. Scuseria, M. A. Robb, J. R. Cheeseman, J. A. Montgomery, Jr., T. Vreven, K. N. Kudin, J. C. Burant, J. M. Millam, S. S. Iyengar, J. Tomasi, V. Barone, B. Mennucci, M. Cossi, G. Scalmani, N. Rega, G. A. Petersson, H. Nakatsuji, M. Hada, M. Ehara, K. Toyota, R. Fukuda, J. Hasegawa, M. Ishida, T. Nakajima, Y. Honda, O. Kitao, H. Nakai, M. Klene, X. Li, J. E. Knox, H. P. Hratchian, J. B. Cross, C. Adamo, J. Jaramillo, R. Gomperts, R. E. Stratmann, O. Yazyev, A. J. Austin, R. Cammi, C. Pomelli, J. W. Ochterski, P. Y. Ayala, K. Morokuma, G. A. Voth, P. Salvador, J. J. Dannenberg, V. G. Zakrzewski, S. Dapprich, A. D. Daniels, M. C. Strain, O. Farkas, D. K. Malick, A. D. Rabuck, K. Raghavachari, J. B. Foresman, J. V. Ortiz, Q. Cui, A. G. Baboul, S. Clifford, J. Cioslowski, B. B. Stefanov, G. Liu, A. Liashenko, P. Piskorz, I. Komaromi, R. L. Martin, D. J. Fox, T. Keith, M. A. Al-Laham, C. Y. Peng, A. Nanayakkara, M. Challacombe, P. M. W. Gill, B. Johnson, W. Chen, M. W. Wong, C. Gonzalez, J. A. Pople, Gaussian, Inc., Wallingford CT, **2004**.

[26] W. J. Hehre, L. Radom, P. von R. Schleyer, J. A. Pople, *Ab Initio Molecular Orbital Theory*, Wiley, New York, **1986**.

[27] a) J. P. Perdew, K. Burke, M. Ernzerhof, *Phys. Rev. Lett.* **1997**, *78*, 1396; b) J. P. Perdew, *Phys. Rev. B* **1986**, *33*, 8822.

[28] a) A. D. Becke, *J. Chem. Phys.* **1993**, *98*, 5648; b) B. Miehlich, A. Savin, H. Stoll, H. Preuss, *Chem. Phys. Lett.* **1989**, *157*, 200; c) C. Lee, W. Yang, G. Parr, *Phys. Rev. B* **1988**, *37*, 785.

[29] a) T. H. Dunning, Jr., P. J. Hay, *Modern Theoretical Chemistry, Vol. 3* (Ed.: H. F. Schaefer III), Plenum Press, New York, **1976**, p. 1; b) P. J. Hay, W. R. Wadt, *J. Chem. Phys.* **1985**, *82*, 270; c) W. R. Wadt, P. J. Hay, *J. Chem. Phys.* **1985**, *82*, 284; d) P. J. Hay, W. R. Wadt, *J. Chem. Phys.* **1985**, *82*, 299.

[30] A. W. Ehlers, M. Böhme, S. Dapprich, A. Gobbi, A. Höllwarth, V. Jonas, K. F. Köhler, R. Stegmann, A. Veldkamp G. Frenking, *Chem. Phys. Lett.* **1993**, *208*, 111.

[31] a) R. Ditchfield, W. J. Hehre, J. A. Pople, *J. Chem. Phys.* **1971**, *54*, 724; b) W. J. Hehre, R. Ditchfield, J. A. Pople, *J. Chem. Phys.* **1972**, *56*, 2257; c) P. C. Hariharan, J. A. Pople, *Mol. Phys.* **1974**, *27*, 209; d) M. S. Gordon, *Chem. Phys. Lett.* **1980**, *76*, 163; e) P. C. Hariharan, J. A. Pople, *Theor. Chim. Acta* **1973**, *28*, 213.

[32] a) C. Peng, P. Y. Ayala, H. B. Schlegel, M. J. Frisch, *J. Comput. Chem.* **1996**, *17*, 49; b) C. Peng, H. B. Schlegel, *Isr. J. Chem.* **1993**, *33*, 449.

[33] a) J. E. Carpenter, F. Weinhold, *THEOCHEM* **1988**, *169*, 41; b) J. E. Carpenter, Ph.D. Thesis, University of Wisconsin (Madison), **1987**; c) J. P. Foster, F. Weinhold, *J. Am. Chem. Soc.* **1980**, *102*, 7211; d) A. E. Reed, F. Weinhold, *J. Chem. Phys.* **1983**, *78*, 4066; e) A. E. Reed, F. Weinhold, *J. Chem. Phys.* **1983**, *78*, 1736; f) A. E. Reed, R. B. Weinstock, F. Weinhold, *J. Chem. Phys.* **1985**, *83*, 735; g) A. E. Reed, L. A. Curtiss, F. Weinhold, *Chem. Rev.* **1988**, *88*, 899; h) F. Weinhold, J. E. Carpenter, *The Structure of Small Molecules and Ions*, Plenum Press, New York, **1988**, p. 227.

[34] MOLEKEL 4.0, P. Flükiger, H. P. Lüthi, S. Portmann, J. Weber, Swiss Center for Scientific Computing, Manno, Switzerland, **2000**.

Received: December 2, 2009
Published online: April 13, 2010

